The Journal of Fourier Analysis and Applications
Volume 8, Issue 4, 2002

A Time Domain Characterization of the Fine Local Regularity of Functions

K.M. Kolwankar and J. Lévy Véhel

Communicated by Guido Weiss

ABSTRACT. We define new functional spaces designed to measure the fine local regularity of functions. In contrast with classical approaches based on, e. g., Littlewood–Paley or wavelet analysis, these spaces are characterized by conditions expressed in the time domain. This is in some cases simpler and more convenient. In particular, because no pre-processing of the data is necessary, it is possible to obtain robust numerical estimation procedures in the case of sampled signals.

1. Introduction

Characterizing the local regularity of functions is an important task in many areas, both in mathematics (e. g., in PDE theory [2] and in applications, for instance in signal processing [4]. The most simple way of doing so is to consider the *pointwise Hölder exponent*. As is well known, this exponent, though a powerful measure of the local regularity, has a number of drawbacks; for example, it is not sensitive to oscillatory behaviors. The *local Hölder exponent* provides a complementary information, which is also useful but partial. A much more complete description is obtained through 2-microlocal analysis, where an infinite set of exponents is used. The 2-microlocal spaces $C^{s,s'}$ are characterized by conditions on the Littlewood–Paley or the wavelet decomposition of the function. Such characterizations are sometimes inconvenient, and they do not lead easily to robust estimation procedures: given a sampled signal, it is not an easy task to compute numerically the associated 2-microlocal exponents.

We propose in this paper a time domain characterization of the fine local regularity structure of functions. The spaces $K^{s,s'}$ we define are similar in spirit to the 2-microlocal spaces (we show in [7] that they do coincide in a certain region of the (s, s') plane), but they

Math Subject Classifications. 26A16, 28A80, 42C40, 60G35.
Keywords and Phrases. 2-microlocal spaces, Hölder exponents, fractals, wavelets, numerical estimation.

ISSN 1069-5869

are simpler to deal with in many respects. For instance, proofs of corresponding results are more elementary for $K^{s,s'}$ spaces than they are for $C^{s,s'}$ spaces (see Section 2). More importantly, they lend themselves more easily to estimation procedures, as we show below.

We recall in Section 2 the definitions of Hölder exponents and 2-microlocal spaces. Section 3 defines and studies the $K^{s,s'}$ spaces. In Section 4 we explain in detail an estimation method and show on various test signals that it yields good results. We believe this opens the way to the actual use of such fine regularity characterizations in applications in signal and image processing. Complementary results dealing with the comparison of $C^{s,s'}$ and $K^{s,s'}$ spaces from both the analytic and numerical point of views are presented in [7].

2. Measures of Local Regularity

In this section we review briefly some of the existing notions of local regularity. These concepts will be useful in Section 3.

2.1 Pointwise Hölder Exponent

Definition 1. Let α be a positive real number which is not an integer, and $x_0 \in \mathbb{R}$. A function $f : \mathbb{R} \to \mathbb{R}$ is in $C^{\alpha}_{x_0}$ if there exists a polynomial P_{x_0} of degree less than α such that:

$$|f(x) - P_{x_0}(x)| \leq c|x - x_0|^{\alpha} . \tag{2.1}$$

When $\alpha \in (0, 1)$, this reduces to:

$$|f(x) - f(x_0)| \leq c|x - x_0|^{\alpha} . \tag{2.2}$$

The pointwise Hölder exponent of f at x_0, denoted $\alpha_p(x_0)$, is the supremum of the α-s for which (2.1) holds. Extension to higher dimensions is straightforward, but will not be considered here.

2.2 Local Hölder Exponent

The local Hölder exponent α_l measures slightly different features as compared to α_p. It is defined as follows: Let $\alpha \in (0, 1)$, $\Omega \subset \mathbb{R}$. One classically says that $f \in C^{\alpha}_l(\Omega)$ if:

$$\exists C : \forall x, y \in \Omega : \frac{|f(x) - f(y)|}{|x - y|^{\alpha}} \leq C .$$

Then, let:

$$\alpha_l (f, x_0, \rho) = \sup \left\{ \alpha : f \in C^{\alpha}_l (B (x_0, \rho)) \right\} .$$

Note that $\alpha_l (f, x_0, \rho)$ is non increasing as a function of ρ. We may now give the definition of the local Hölder exponent:

Definition 2. Let f be a continuous function. The local Hölder exponent of f at x_0 is the real number:

$$\alpha_l (f, x_0) = \lim_{\rho \to 0} \alpha_l (f, x_0, \rho) .$$

Contrarily to α_p, α_l is stable under pseudo-differentiation or integration. Its main drawback is that it is not as precise as α_p in the following sense: the class of pointwise Hölder functions (i. e., functions $x \to \alpha_p(f, x)$) of continuous functions f coincides with that of $liminf$ of continuous functions, while local Hölder functions must be lower semi-continuous. Thus, for instance, one cannot observe, using α_l, a "regular" isolated point in an "irregular" environment, while this is possible when one uses α_p (see [3] and [4]).

Some important differences between α_p and α_l are well illustrated on the example of the chirp $f(x) = |x|^\beta \cos(1/|x|^\gamma)$, $f(0) = 0$, with $\beta, \gamma > 0$. In this case, at $x = 0, \alpha_p = \beta$ while $\alpha_l = \frac{\beta}{1+\gamma}$. Thus, while α_p is sensitive only to what happens "at" 0, α_l measures also the local oscillatory behavior of the signal "around" 0. Moreover, the pointwise exponent for a primitive of f is $\beta + 1 + \gamma$, while the local one is just $\frac{\beta}{1+\gamma} + 1$.

Limitations of both α_p and α_l call for a generalized frame, which is provided by 2-microlocal spaces.

2.3 2-Microlocal Spaces

The original definition of the 2-microlocal spaces [2] is based on a Littlewood–Paley analysis, that we recall for convenience. Let $\mathcal{S}(\mathbb{R})$ be the Schwartz space and define:

$$\varphi \in \mathcal{S}(\mathbb{R}) = \left\{ \begin{array}{l} \widehat{\varphi}(\xi) = 1, \parallel \xi \parallel < \frac{1}{2} \\ \widehat{\varphi}(\xi) = 0, \parallel \xi \parallel > 1 \end{array} \right. ,$$

and

$$\varphi_j(x) = 2^j \varphi \left(2^j x \right) .$$

One has

$$\widehat{\varphi}_j(\xi) = \widehat{\varphi} \left(2^{-j} \xi \right) .$$

The $\{\varphi_j\}$ set acts as low pass filter bank, which leads naturally to the associated band pass filter bank:

$$\psi_j = \varphi_{j+1} - \varphi_j .$$

Definition 3. Let $u \in \mathcal{S}'(\mathbb{R})$. The Littlewood–Paley Analysis of u is the set of distributions:

$$\left\{ \begin{array}{lcl} S_0 u & = & \varphi * u \\ \Delta_j u & = & \psi_j * u \end{array} \right. .$$

One has:

$$u = S_0 u + \sum_{j=0}^{\infty} \Delta_j u.$$

We can now define the two microlocal spaces $C_{x_0}^{s,s'}$.

Definition 4 ([2]). A distribution $u \in \mathcal{S}'(\mathbb{R})$ belongs to the 2-microlocal space $C_{x_0}^{s,s'}$ if there exists a positive constant c such that, for all j:

$$\left\{ \begin{array}{l} |S_0 u(x)| \leq c(1 + |x - x_0|)^{-s'} \\ |\Delta_j u(x)| \leq c 2^{-js} \left(1 + 2^j |x - x_0|\right)^{-s'} \end{array} \right. .$$

The 2-microlocal spaces are related to the pointwise Hölder spaces through:

Theorem 1 ([5]).

$\forall x_0 \in \mathbb{R}$, $\forall s > 0$*:*

- $C^s_{x_0} \subset C^{s,-s}_{x_0}$.
- $C^{s,s'}_{x_0} \subset C^s_{x_0}, \forall s + s' > 0$.

For a given f, we may associate to each point x_0 its *2-microlocal domain*, i. e., the subset of $\mathbb{R} \times \mathbb{R}$ of couples (s, s') such that $f \in C^{s,s'}_{x_0}$. It is easy to show that $f \in C^{s,s'}_{x_0}$ implies that $f \in C^{s-\epsilon,s'+\epsilon}_{x_0}$ for all positive ϵ. This induces a particular shape for the frontier of the 2-microlocal domain:

Definition and Proposition 1 (2-microlocal frontier parametrization [4]).

Let $f : \mathbb{R} \to \mathbb{R}$, and define, for a given x_0,

$$S\left(s', x_0\right) \quad = \quad \sup\left\{s : f \in C^{s,s'}_{x_0}\right\} .$$

The 2-microlocal frontier of f at x_0 is the set of points

$$\Gamma(f, x_0) \quad = \quad \left\{\left(S(s'), s'\right)\right\} .$$

The function $S(., x_0)$ is decreasing and convex. Moreover, one has, for all positive τ:

$$S(\sigma + \tau, x_0) \geq S(\sigma, x_0) - \tau .$$

By slight abuse of notation, we shall call $S(\sigma, x_0) = S(\sigma)$ the 2-microlocal frontier. The 2-microlocal spaces generalize the Hölder spaces and allow to re-interpret both α_l and α_p:

Proposition 1.

For all x, we have :

$$\alpha_l(x) = S(0, x) .$$

If $\sup_{\epsilon>0} S(\epsilon) > 0$*, then*

$$\alpha_p(x) = \sigma_0(x)$$

where $\sigma_0(x)$ is the unique value for which

$$S(-\sigma_0, x) = \sigma_0 .$$

In other words, α_l is obtained as the intersection between the 2-microlocal frontier and the s-axis, while α_p is the intersection between the 2-microlocal frontier and the line $s' = -s$, provided $\sup_{\epsilon>0} S(\epsilon) > 0$. This last relation holds if f has some minimum overall regularity, i. e., for instance f belongs to the global Hölder space C^ω for some positive ω.

Finally, we recall that a major motivation for studying 2-microlocal spaces is that they behave well under differentiation:

Proposition 2 ([6]).

$$f \in C^{s,s'}_{x_0} \quad \textit{iff} \quad \frac{df}{dx} \in C^{s-1,s'}_{x_0} .$$

In fact, more is true, as pseudo-differential operators may be considered instead of plain differentials.

3. The Spaces $K_{x_0}^{s,s'}$

In this section, we show how to combine, purely in the "time domain," the information conveyed by the local and pointwise Hölder exponents. In that view, we define new functional spaces that characterize finely the local regularity. These provide an alternative approach to 2-microlocal spaces, that is perhaps simpler in certain respects.

Definition 5. A function $f : I \subset \mathbb{R} \to \mathbb{R}$ belongs to $K_{x_0}^{s,s'}$ if, for some $0 < \delta < 1/4$, $C > 0$, and for all (x, y) satisfying $|x - x_0| < \delta$ and $|y - x_0| < \delta$, the following estimate holds:

$$|f(x) - f(y)| \leq C|x - y|^{s+s'} (|x - y| + |x - x_0|)^{-s'/2} (|x - y| + |y - x_0|)^{-s'/2} \quad . \tag{3.1}$$

Remark 1: One can equivalently use an asymmetric version of the above inequality, i. e.,

$$|f(x) - f(y)| \leq C|x - y|^{s+s'} (|x - y| + |x - x_0|)^{-s'} \quad .$$

Remark 2: Since the definition uses first order differences, it is easy to see that it does not make sense to consider values larger than 1 for both s and $-s'$. This version is thus relevant only for the study of non smooth functions. Extension to higher order singularities is possible if one replaces $|f(x) - f(y)|$ by corresponding higher order differences, or by introducing a polynomial as in (2.1). We deal with such an extension in [7]. Likewise, the definition of $K^{s,s'}$ only makes sense for functions, where pointwise values are well defined. In order to extend it to distributions, one could for instance consider (iterated) integrals.

Proposition 3.

If $f \in K_{x_0}^{s,s'}$ and if t and t' are such that $t < s$ and $t + t' < s + s'$ then $f \in K_{x_0}^{t,t'}$.

Proof. We have two cases:

(i) $t' < s'$: This is obvious from the definition.

(ii) $t' \geq s'$: In this case we can write

$$\begin{aligned} &|x - y|^{s+s'}(|x - y| + |x - x_0|)^{-s'/2}(|x - y| + |y - x_0|)^{-s'/2} \\ &\quad \leq |x - y|^{t+t'}(|x - y| + |x - x_0|)^{-t'/2}(|x - y| + |y - x_0|)^{-t'/2} \, . \end{aligned}$$ □

Let $D(f, x_0)$ be the planar set consisting of all pairs $(s, s') \in \mathbb{R}^2$ such that $f(x) \in K_{x_0}^{s,s'}$. Let us denote by Γ the boundary of $D(f, x_0)$. It follows from Proposition 3 that Γ is the graph $s = A(s')$ of a function which is decreasing and $A(s') - \tau \leq A(s' + \tau)$ for $\tau > 0$. It is easily shown that this frontier is a convex function, hereafter referred to as the "K-frontier."

Proposition 4.

$\forall s \geq 0, C_{x_0}^s \subset K_{x_0}^{s,-s}$

Proof. If $f(x) \in C^s_{x_0}$ we have

$$\begin{aligned}
|f(x) - f(y)| &\leq |f(x) - f(x_0)| + |f(y) - f(x_0)| \\
&\leq C\left(|x - x_0|^s + |y - x_0|^s\right) \\
&\leq C\left[(|x - y| + |y - x_0|)^s + (|x - y| + |x - x_0|)^s\right] \\
&= C\,(|x - y| + |y - x_0|)^{s/2}\,(|x - y| + |x - x_0|)^{s/2} \\
&\qquad \left[\left(\frac{|x - y| + |y - x_0|}{|x - y| + |x - x_0|}\right)^{s/2} + \left(\frac{|x - y| + |x - x_0|}{|x - y| + |y - x_0|}\right)^{s/2}\right] \\
&\leq C'\,(|x - y| + |y - x_0|)^{s/2}\,(|x - y| + |x - x_0|)^{s/2}\ .
\end{aligned}$$

The last inequality shows that $f(x) \in K^{s,-s}_{x_0}$. □

All the properties of the spaces $K^{s,s'}_{x_0}$ discussed so far are shared by their 2-microlocal counterpart. The following proposition highlights one of the crucial differences between the two types of spaces.

Proposition 5.
For all (s, s'), $K^{s,s'}_{x_0} \subset C^s_{x_0}$.

Proof. Setting $y = x_0$ in Definition 5 yields:

$$|f(x) - f(x_0)| \leq C|x - x_0|^s\ . \qquad \square \tag{3.2}$$

Remark 3: From Propositions 4 and 5, it follows that, for $s \geq 0$, $K^{s,s'}_{x_0} \subset C^s_{x_0} \subset K^{s,-s}_{x_0}$. This in turn implies that for all $s \geq 0$ and for all s', $K^{s,s'}_{x_0} \subset K^{s,-s}_{x_0}$. Also, Proposition 3 gives us that $K^{s,-s}_{x_0} \subset K^{s,s''}_{x_0}$ for $s'' < -s$. These two facts imply a peculiar property of the spaces $K^{s,s'}_{x_0}$: $K^{s,s'}_{x_0} = K^{s,s''}_{x_0}$ for s', $s'' < -s$. Graphically this means that, in the (s, s')-plane, "after" the frontier crosses the line $s + s' = 0$, it takes the form $s = c$, where the constant c is the abscissa of the point where the frontier crosses the $s + s' = 0$ line. Such a property does not hold in general for 2-microlocal frontiers.

The following two propositions show that both the pointwise and local Hölder exponents can be read off from the frontier. The results are same as the ones for $C^{s,s'}$ spaces, but the analysis is simpler.

Proposition 6.
$A(0) = \alpha_l(x_0)$.

Proof. It is clear from the definition of $K^{s,s'}_{x_0}$ that if we substitute $s' = 0$ then f satisfies the inequality

$$|f(x) - f(y)| \leq C|x - y|^s \tag{3.3}$$

which is nothing but the Hölder condition. This implies that $f \in C^s_{B(x_0,\delta)}\ \forall\delta$. In particular, if we take the limit $\delta \to 0$ this implies $s \leq \alpha_l(x_0)$. The supremum over all such s is, by definition, $\alpha_l(x_0)$. Also by the definition of $A(s)$ this supremum is equal to $A(0)$. □

Proposition 7.
If $A(0) = \alpha > 0$ and $\alpha_p(x_0) \leq 1$, then $\alpha_p(x_0)$ is the unique $t > 0$ such that $A(-t) = t$.

Proof. Because of Remark 2, we know that the frontier can not cross to the right of $s = 1$ in the (s, s')-plane. Together with the fact that $A(0) > 0$, this implies the existence and uniqueness of t such that $A(-t) = t$. Now, if $A(-\gamma) = \gamma$ then for a given $s < \gamma$ we can find s' such that $f(x) \in K_{x_0}^{s,s'}$. Therefore the supremum over such s is γ. By Proposition 5 we have $K_{x_0}^{s,s'} \subset C_{x_0}^{s}$. This implies that $\gamma \leq \alpha_p(x_0)$. Now by Proposition 4 we have $C_{x_0}^{s} \subset K_{x_0}^{s,-s}$. This implies that $\alpha_p(x_0) \leq \gamma$. □

This determines the constant c in Remark 3 above: Proposition 7 implies that, once the frontier crosses the line $s + s' = 0$, it is described by the equation $s = \alpha_p(x_0)$.

The behavior of the frontier in the quadrant where both s and s' are positive depends upon the regularity of the function in the excluded neighborhood of x_0. This property is special to this version of $K^{s,s'}$ spaces, and is not shared by 2-microlocal spaces. The result can be stated as follows:

Proposition 8.

Let $\tilde{\alpha} = \min(1, \lim_{\delta \to 0} \inf_{x_0 \neq x \in B(x_0,\delta)} \alpha_p(x))$. *If* $s + s' > \tilde{\alpha}$ *then* $(s, s') \notin D(f, x_0)$.

Proof. $\forall y, \forall \epsilon > 0, \exists (x_i)_i$ s. t. $x_i \to y$ as $i \to \infty$ and $|f(x_i) - f(y)| \leq C|x_i - y|^{\alpha_p(y)-\epsilon}$. Therefore for any given $y \neq x_0$, the ratio

$$\frac{|f(x_i) - f(y)|}{|x_i - y|^{s+s'} \left(|x_i - y| + |x_i - x_0|\right)^{-s'/2} \left(|x_i - y| + |y - x_0|\right)^{-s'/2}}$$

goes to ∞ with i if $s + s' > \alpha_p(y)$. If the function is smooth at all points in a neighborhood of x_0, except at x_0, then it is locally Lipschitz and we have that the frontier can not cross to the right of the line $s + s' = 1$. □

Note that since $\tilde{\alpha}$ is always larger than α_l, there is no contradiction with the fact that the frontier passes through the point $(0, \alpha_l)$. Summing up what has been proved so far, we have that the generic shape of a K- frontier is as shown in Figure 1. We see that the part that really carries information is the one between the two parallel lines $s + s' = 0$ and $s + s' = \tilde{\alpha}$. We show in [7] that, in this region, $K^{s,s'} = C^{s,s'}$ (in fact, one has equality on a larger domain, provided a generalized definition of $K^{s,s'}$ spaces is used). Thus, for the range of values where $K^{s,s'}$ spaces are meaningful, they can serve as exact, pure time domain, substitutes for 2-microlocal spaces (in particular, they allow to predict the shift in pointwise regularity under pseudo-differentiation of "small" order). Note finally that, by making use of the extension in the definition of $K^{s,s'}$ spaces given in [7], one can extend the meaningful region to the set $\{(s, s'), s + s' > 0, s > 0, s' < 0\}$.

Example: In order to give some feeling about $K^{s,s'}$ spaces, we compute the K-frontier of a chirp $f(x) = |x|^{\gamma} \sin(2\pi/|x|^{\beta})$, $0 < \gamma < 1$ and $\beta > 0$. We show, in agreement with the theoretical results above, that, for $s' < 0$, the frontier at $x_0 = 0$ is given by the line $(\beta + 1)s + \beta s' = \gamma$ for $s' > -\gamma$ and by $s = \gamma$ for $s' < -\gamma$.

Define sequences $(x_k)_{k \in \mathbb{N}}$ and $(y_k)_{k \in \mathbb{N}}$ as follows:

$$x_k^{\beta} = \frac{4}{4k+1} \quad \text{and} \quad y_k^{\beta} = \frac{4}{4k+3}\,. \tag{3.4}$$

We have

$$f(x_k) = \left(\frac{4}{4k+1}\right)^{\frac{\gamma}{\beta}}, \quad f(y_k) = -\left(\frac{4}{4k+3}\right)^{\frac{\gamma}{\beta}}\,. \tag{3.5}$$

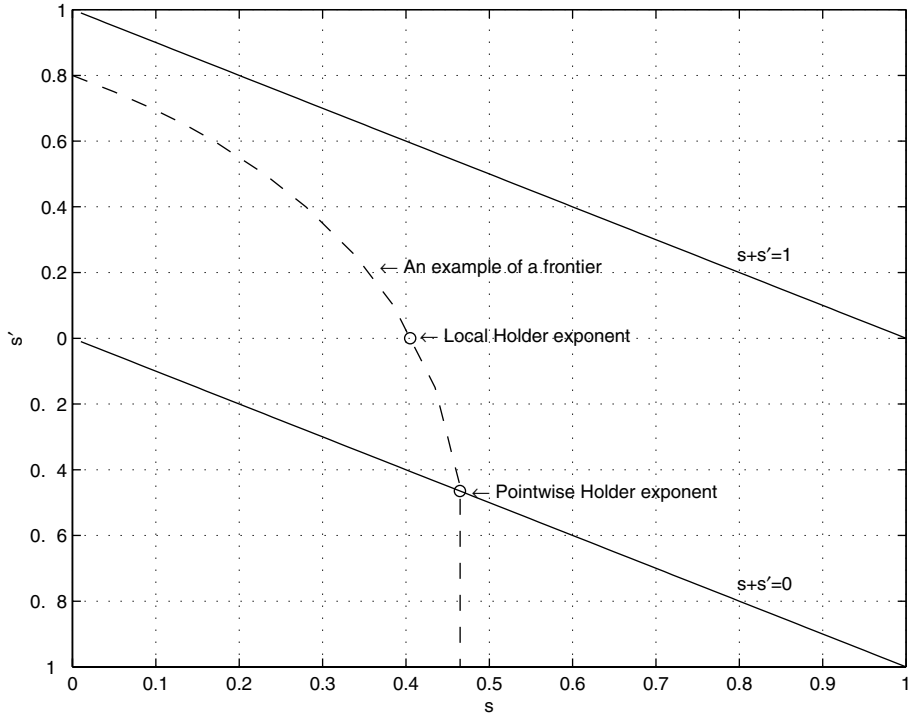

FIGURE 1 The generic shape of a frontier.

When k is large,

$$\begin{aligned} x_k \sim k^{\frac{-1}{\beta}}, \quad y_k &\sim k^{\frac{-1}{\beta}}, \\ |x_k - y_k| &\sim k^{\frac{-\beta+1}{\beta}}, \\ |f(x_k) - f(y_k)| &\sim k^{\frac{-\gamma}{\beta}} \end{aligned}$$

and

$$|x_k - y_k|^{s+s'} \left(|x_k - y_k| + |x_k|\right)^{-s'/2} \left(|x_k - y_k| + |y_k|\right)^{-s'/2} \sim k^{\frac{-s(\beta+1)-s'\beta}{\beta}}. \tag{3.6}$$

This shows that the ratio

$$\frac{|f(x_k) - f(y_k)|}{|x_k - y_k|^{s+s'} \left(|x_k - y_k| + |x_k|\right)^{-s'/2} \left(|x_k - y_k| + |y_k|\right)^{-s'/2}} \tag{3.7}$$

will go to ∞ as $k \to \infty$ along the sequences (x_k), (y_k), whenever $(\beta+1)s + \beta s' > \gamma$. In other words, if a pair (s, s') satisfies this inequality, then $f \notin K_0^{s,s'}$.

In order to ensure that this indeed is the frontier for $-\gamma < s' < 0$, we have to show that the ratio in (3.7) remains bounded for all x and y. There are two limiting cases: (i) $|x - y|$ is small compared to $|x|$ and (ii) $|x|$ or $|y|$ is small compared to $\max(|x|, |y|)$. Without loss of generality we assume $0 < y < x$ and begin with the first case. We show that for $-\gamma < s' < 0$ and $x - x^{\beta+1} \leq y < x$,

$$\frac{|f(x) - f(y)|}{|x - y|^{s+s'} \left(|x - y| + |x|\right)^{-s'/2} \left(|x - y| + |y|\right)^{-s'/2}} \leq K \tag{3.8}$$

if $(\beta+1)s+\beta s' \le \gamma$. It is easily seen that $|f'(t)| \le Cy^{\gamma-\beta-1}$ for $t \in [y, x]$. Thus:

$$\begin{aligned}
&\frac{|f(x)-f(y)|}{|x-y|^{s+s'}\,(|x-y|+|x|)^{-s'/2}\,(|x-y|+|y|)^{-s'/2}} \\
&\quad\le \frac{Cy^{\gamma-\beta-1}}{|x-y|^{s+s'-1}\,(|x-y|+|x|)^{-s'/2}\,(|x-y|+|y|)^{-s'/2}} \\
&\quad\le \frac{Cy^{\gamma-\beta-1}}{|x-y|^{s+s'-1}\,(|x-y|+|y|)^{-s'}} \\
&\quad\le Cy^{\gamma-\beta-1+s'}|x-y|^{-s+1-s'} \\
&\quad\le Cy^{\gamma-\beta-1+s'}x^{(\beta+1)(-s+1-s')}\,.
\end{aligned}$$

Therefore we get the result. Now consider the second case. We have:

$$\begin{aligned}
\frac{|f(x)-f(y)|}{|x-y|^{s+s'}\,(|x-y|+|x|)^{-s'/2}\,(|x-y|+|y|)^{-s'/2}} &\sim \frac{|f(x)|}{|x|^s 2^{-s'/2}} \\
&\le K
\end{aligned}$$

if $s < \gamma$ since $|f(x)| \le |x|^\gamma$. Since $\gamma > (\beta+1)s+\beta s'$ in the range $-\gamma < s' < 0$, it follows that in this range the frontier is given by $(\beta+1)s+\beta s' = \gamma$. From the properties of the frontier, it follows that the frontier for $s' < -\gamma$ is given by $s = \gamma$.

4. Numerical Estimation of the K-Frontier

An advantage of $K^{s,s'}$ spaces is that they provide a purely temporal characterization of the fine local regularity of functions. While frequency or wavelet based characterizations are in many cases equally or more convenient, we have seen above that some analytical properties are easier to prove in the time domain. In addition, as we show now, such an approach allows to design a simple and efficient numerical algorithm to estimate the K-frontier.

4.1 Definition of the Estimator

In this section we develop a numerical algorithm that determines the frontier $K(f, x_0)$ of a function f at a given point x_0. We assume given $2M+1$ samples of f and we denote by f_i the value of the function at $x = x_i$, where i is an integer ranging in $[-M, M]$. Note that we need not require that the samples are equispaced. Fix $N \le M$, and write, for $i \ne j$, $i, j \in [-N, N]$,

$$C_{ij}\left(s, s'\right) = \frac{|f_i - f_j|}{|x_i - x_j|^{s+s'}(|x_i - x_j| + |x_i - x_0|)^{-s'/2}(|x_i - x_j| + |x_j - x_0|)^{-s'/2}}\,.$$

Now define, for $n = 1 \ldots N$,

$$R\left(n, s_k, s'_l\right) = \max_{-n \le i < j \le n} C_{ij}\left(s_k, s'_l\right) \tag{4.1}$$

where s_k and s'_l are discretized values of s and s' respectively. The couples (s_k, s'_l) are the points of the (s,s') plane where we shall perform the estimation.

For a given value of s'_l, we expect that if $s_k < A(s'_l)$ then $R(n, s_k, s'_l)$ is small for small n and increases with n, whereas it should remain constant if $s_k > A(s'_l)$. This is demonstrated in Figure 2(a) in the case of $f(x) = |x|^\gamma$. However for more complex functions, in particular oscillating ones, one cannot hope that such a behavior will hold in general, due to various factors, the main one being discretization effects. Whereas $R(n, s_k, s'_l)$ is still a nondecreasing function of n when $s_k < A(s'_l)$, it is not a constant function in the second case, when $s_k > A(s'_l)$. In this case $R(n, s_k, s'_l)$ is small for small n but it increases faster and saturates after some value of n depending on the sampling rate. This is demonstrated in Figure 2(b) in the case of a chirp. Set

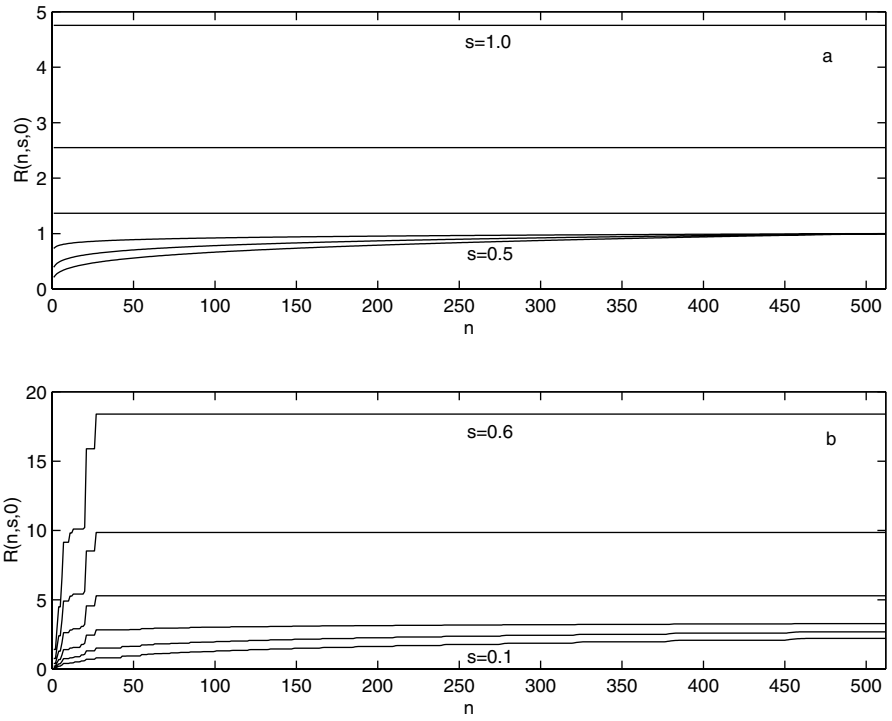

FIGURE 2 Plot of $R(n, s, s' = 0)$ vs. n for (a) $f(x) = |x|^\gamma$,$\gamma = 0.75$, $s = 0.5, 0.6, \ldots, 1.0$ and (b) $f(x) = |x|^\gamma \sin(1/|x|^\beta)$, $\gamma = 0.5$, $\beta = 0.5$ and $s = 0.1, 0.2, \ldots, 0.6$.

$$L\left(s_k, s'_l\right) = N - \max\left\{n : R\left(n, s_k, s'_l\right) \neq R\left(N, s_k, s'_l\right)\right\} . \tag{4.2}$$

This gives the length of the plateau with maximum value of $R(n, s_k, s'_l)$ for given values of s_k and s'_l. Plot of $L(s_k, s'_l)$ for simple functions [Figures 3(a) and 3(b)] shows that it has a strong discontinuity at the critical value of s_k, i. e., when $s_k = A(s'_l)$. In order to find this critical s in general, we look for a jump in $L(s_k, s'_l)$. Therefore we define our estimator $\hat{A}(s'_l)$ to be $\hat{A}(s'_l) = s_{cr}$ where $s_{cr} = \max\{s_k : L(s_{k+3}, s'_l) - L(s_k, s'_l)$ is maximum$\}$. It turns out that, due to numerical limitations, the estimated frontier $\hat{A}(s')$ thus obtained is not always concave. Therefore we take its double Legendre transform to remove minor oscillations and obtain a concave curve. This defines our estimator.

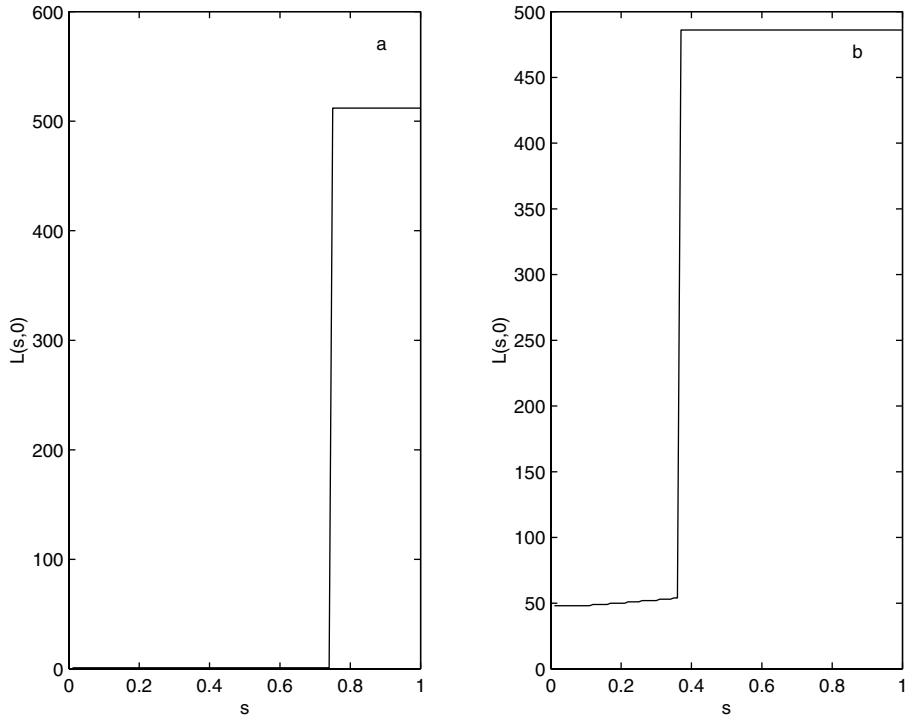

FIGURE 3 Plot of $L(s, s' = 0)$ vs. s for (a) $f(x) = |x|^\gamma$, $\gamma = 0.75$ and (b) $f(x) = |x|^\gamma \sin(1/|x|^\beta)$, $\gamma = 0.5$ and $\beta = 0.5$.

4.2 Numerical Experiments

We apply the procedure above to estimate the frontiers of various sampled functions. We start with the simple cases of power laws and chirps, then move to sum of chirps, where there are two competing oscillatory behaviors. Next, we consider the case of nowhere differentiable functions : fractional Brownian motion is our example in the case of stochastic processes, and we choose the Weierstrass function for the deterministic case. Finally, we deal with the important case of functions that have non constant Hölder regularity. The first one is a generalized Weierstrass function with smoothly varying pointwise and local exponents. The second one is the graph of an IFS, which is multifractal and thus has wildly varying pointwise Hölder exponents. All results are given for signals of modest size, i. e., 1025 points.

4.2.1 Power Laws and Chirps

The results for a power law and a chirp are presented in Figure 4. One can see that the estimated frontier perfectly matches the theoretical one. Note that, even for a single chirp, and to the best of our knowledge, there is no (other) algorithm which allows to evaluate the 2-microlocal frontier.

4.2.2 Sum of Chirps

The following lemma is obvious:

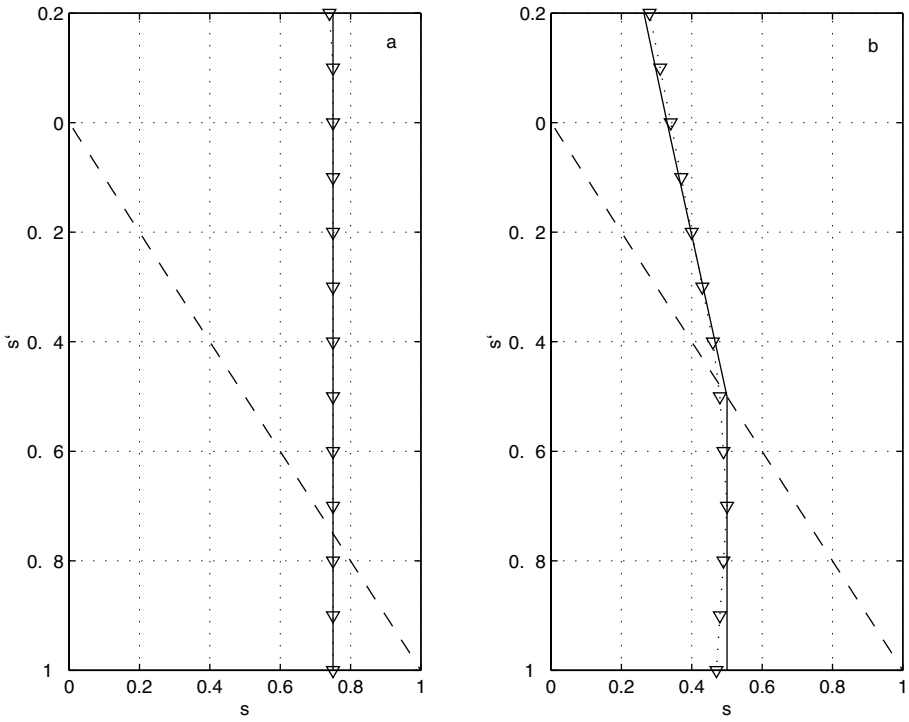

FIGURE 4 Frontier $s = A(s')$ for (a) $f(x) = |x|^\gamma$, $\gamma = 0.75$ and (b) $f(x) = |x|^\gamma \sin(1/|x|^\beta)$, $\gamma = 0.5$ and $\beta = 0.5$. The solid line is the theoretical frontier while the triangles connected with dots give the estimated one. The dashed line is the straight line $s' = -s$.

Lemma 1.

Let $f_1 \in K_{x_0}^{s_1,s_1'}$, $f_2 \in K_{x_0}^{s_2,s_2'}$, *and assume that* $(s_1, s_1') \neq (s_2, s_2')$. *Then:* $f_1 + f_2 \in K_{x_0}^{\min(s_1,s_2),\min(s_1',s_2')}$.

We consider the function

$$f(x) = |x|^{\gamma_1} \sin\left(\frac{1}{|x|^{\beta_1}}\right) + |x|^{\gamma_2} \sin\left(\frac{1}{|x|^{\beta_2}}\right) . \tag{4.3}$$

This function has two oscillatory behaviors superimposed on each other. In the region of interest, i. e., above the line $s + s' = 0$ and below the line $s' = 0$, the frontiers of the two components are straight lines. Let us choose the parameters $\gamma_1, \gamma_2, \beta_1, \beta_2$ so that these two lines intersect in the region of interest. From the above lemma, we get that the frontier of f is the "minimum" of these two frontiers. As a consequence, depending on the location (s, s'), one of the individual chirps will dominate. It is interesting to check whether our algorithm is able to detect this "phase transition," i. e., the discontinuous change of slope in the frontier. It can be seen from Figure 5 that it indeed does so satisfactorily. Thus, using $K^{s,s'}$ spaces and the method described above, it is possible to estimate, with reasonable accuracy, frontiers which are not straight lines. Again, detecting such fine local behavior appears to be new in the literature.

For practical applications, it is important to test the method on functions with non isolated singularities. We address this case in the next section.

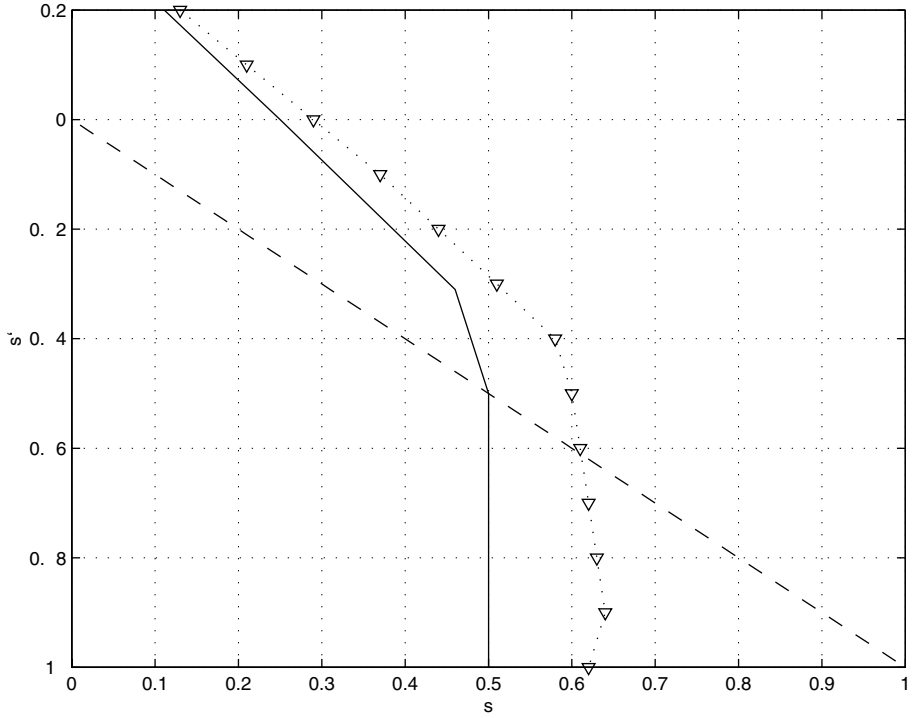

FIGURE 5 Frontier of the sum of two chirps with $\gamma_1 = 0.8$, $\beta_1 = 2.2$, $\gamma_2 = 0.5$ and $\beta_2 = 0.25$. The solid line is the theoretical frontier and the triangles connected with dots represent the estimated one.

4.2.3 Everywhere Singular Functions

We consider here four signals:

- the Weierstrass function, defined as:

$$W_\lambda^h(t) = \sum_{k=0}^{\infty} \lambda^{-hk} \sin\left(\lambda^k t\right) \tag{4.4}$$

  where $\lambda \geq 2$ and $0 < h < 1$. It is well known that this function has everywhere $\alpha_p(t) = \alpha_l(t) = h$.
- a fractional Brownian motion of exponent h (see for instance [1]), for which $\alpha_p(t) = \alpha_l(t) = h$ for all t almost surely.
- the generalized Weierstrass function:

$$W_\lambda^t(t) = \sum_{k=0}^{\infty} \lambda^{-kt} \sin\left(\lambda^k t\right) \tag{4.5}$$

  defined on $(0, 1)$. It is shown for instance in [3] that $\alpha_p(t) = \alpha_l(t) = t$ for all t.
- the graph of an IFS (see [3]). More precisely, we consider a function defined on $[0, 1]$ verifying the functional identity:

$$f(x) = c_1 f(2x) + c_2 f(2x - 1) \tag{4.6}$$

  where $0.5 < |c_1| < |c_2| < 1$. It is known that $\alpha_l(t) = -\log_2(|c_2|)$ for all t. Furthermore, $\alpha_p(t)$ is everywhere discontinuous, and ranges in $[-\log_2(|c_2|), -\log_2$

$(|c_1|)$]. Finally, for all α in this interval, the set of t for which $\alpha_p(t) = \alpha$ is dense in [0, 1]. This is thus an example where the local and pointwise exponents have drastically different behaviors, with a constant α_l and a wildly varying α_p. It may be shown that the theoretical shape of the frontier at any point t is as indicated on the left of Figure 6. It is made of two half lines. The first one with slope -1 crosses the s-axis at the point $(\alpha_l, 0)$ and ends at the point with abscissa α_p. The second one is vertical and of course goes through the point $(\alpha_p, -\alpha_p)$. When t is varied in an interval, α_l does not change while α_p assumes its full range, thus resulting in a set of frontiers as sketched on the right of Figure 6.

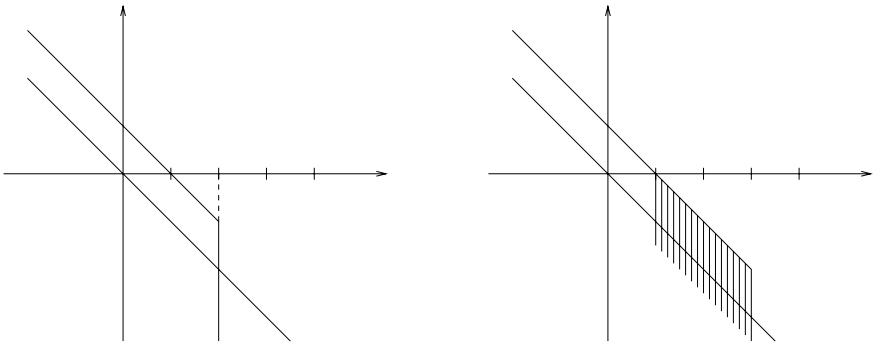

FIGURE 6 Theoretical frontier at a given point of an IFS (left) and set of theoretical frontiers at all points of an IFS (right).

We show in Figure 7 the frontiers estimates at randomly chosen points of these four functions. Even in these notoriously difficult cases, the results are reasonably accurate:

- Weierstrass function
  Note first that the shapes of the frontiers have the right appearance. In particular, they are approximately vertical between $(\alpha_l(t), 0)$ and $(\alpha_p(t), -\alpha_p(t))$. The estimates for α_l vary between 0.42 and 0.61, and for α_p between 0.46 and 0.59. This is not too far from the theoretical 0.5, with a slightly larger dispersion for α_l.
- Fractional Brownian motion
  The same remarks as for the Weierstrass function apply, namely a correct overall shape. The main difference is a larger variance for the estimate of α_l, which ranges in [0.4, 0.6], and a better estimate of α_p, between 0.5 and 0.59.
- Generalized Weierstrass function
  Once again, the overall appearance is close to the theoretical one. However, due to the varying regularity, a bias appears: instead of being vertical below the point $(\alpha_l(t), 0)$, the frontier becomes vertical at the point with ordinate $\simeq -0.2$. In other words, while the pointwise exponent is relatively well estimated, the local one is systematically underestimated. This is easily explained if one realizes that the global exponent of W_λ^t in any ball $B(t, \epsilon)$ of radius ϵ centered at point t is $t - \epsilon$. Since the algorithm works with balls of finite size ϵ, it will at any point t estimate $\hat{\alpha}_l = t - \epsilon$ instead of $\alpha_l = t$.

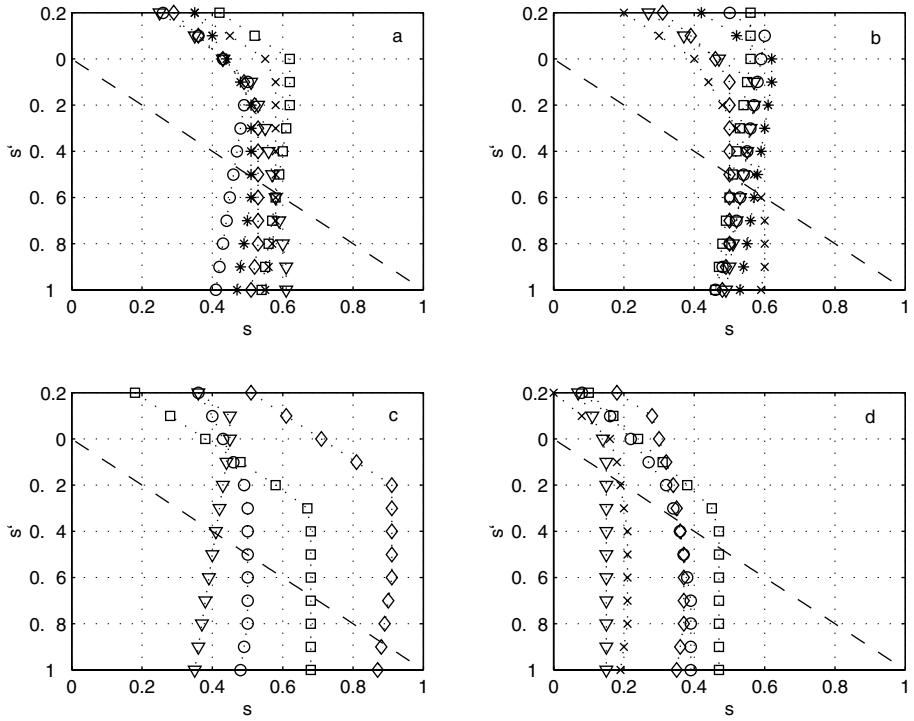

FIGURE 7 Frontiers at randomly selected points of (a) the Weierstrass function with $h = 0.5$, (b) a path of an fBm with $h = 0.5$, (c) the generalized Weierstrass function with Hölder function $h(t) = t$. (d) the graph of an IFS with contraction ratios $c_1 = 0.7$ and $c_2 = 0.9$.

- Graph of an IFS.
  Comparing with Figure 6, we see that the basic shape is roughly correct. The theoretical range for α_p is [0.15, 0.51], which is close to the observed one [0.18, 0.47]. The results are again a bit worse for α_l: it should equal 0.15 at all points, while estimated values vary between 0.17 and 0.3. We do not have, at this point, an explanation for this fact.

Finally, it is interesting to note that all the results are consistent with Proposition 8 in the first quadrant.

This algorithm is implemented in FracLab, a software toolbox available at: www.rocg.inria.fr/fractals.

References

[1] Beran, J. (1994) *Statistics for Long-Memory Processes,* Chapman and Hall.

[2] Bony, J.-M. (1986). Second microlocalization and propagation of singularities for semilinear hyperbolic equations, in *Hyperbolic Equations and Related Topics,* (Katata/Kyoto, 1984), Academic Press, Boston, MA, 11–49.

[3] Daoudi, K., Lévy Véhel, J., and Meyer, Y. (1998). Construction of continuous functions with prescribed local regularity, *J. Constructive Approx.,* **14**(3), 349–385.

[4] Guiheneuf, B. and Lévy Véhel, J. (1998). 2-microlocal analysis and application in signal processing, in *International Wavelets Conference,* Tangier, Inria.

[5] Jaffard, S. and Meyer, Y. (1996). Wavelet methods for pointwise regularity and local oscillations of functions, *Mem. Am. Math. Soc.,* **123**(587), x+110.

[6] Meyer, Y. (1998) *Wavelets, Vibrations and Scalings,* CRM, Vol. 9.

[7] Seuret, S. and Lévy Véhel, J. (2001). A time domain characterization of 2-microlocal spaces, submitted.

Received December 26, 2000

Projet Fractales, INRIA Rocquencourt, B. P. 105, 78153 Le Chesnay Cedex, France

Irccyn, B. P. 92101, 44321 Nantes, France
e-mail: Jacques.Levy_Vehel@inria.fr